PHYSICAL REVIEW E, VOLUME 64, 051807

Dynamics of α and β processes in thin polymer films: Poly(vinyl acetate) and poly(methyl methacrylate)

Koji Fukao,[1,*] Shinobu Uno,[2] Yoshihisa Miyamoto,[1] Akitaka Hoshino,[2] and Hideki Miyaji[2]
[1]*Faculty of Integrated Human Studies, Kyoto University, Kyoto 606-8501, Japan*
[2]*Department of Physics, Kyoto University, Kyoto 606-8502, Japan*

(Received 8 May 2001; published 24 October 2001)

Dynamics of thin films of poly(vinyl acetate) (PVAc) and poly(methyl methacrylate) (PMMA) have been investigated by dielectric relaxation spectroscopy in the frequency range from 0.1 Hz to 1 MHz at temperatures from 263 to 423 K. The α process, the key process of glass transition, is observed for thin films of PVAc and PMMA as a dielectric loss peak at a temperature T_α in temperature domain with a fixed frequency. For PMMA, the β process is also observed at a temperature T_β. For PVAc, T_α decreases gradually with decreasing thickness, and the thickness dependence of T_α is almost independent of the molecular weight ($M_\mathrm{w} \leqslant 2.4 \times 10^5$). For PMMA, T_α remains almost constant as thickness decreases down to a critical thickness d_c, at which point it begins to decrease with decreasing thickness. Contrastingly, T_β decreases gradually as thickness decreases to d_c, and below d_c it decreases drastically. For both PVAc and PMMA, the broadening of the distribution of the relaxation times in thinner films is observed and this broadening is more pronounced for the α process than for the β process. It is also observed that the relaxation strength is depressed as the thickness decreases for both the polymers.

DOI: 10.1103/PhysRevE.64.051807 PACS number(s): 64.70.Pf, 68.60.−p, 77.22.Gm

I. INTRODUCTION

Recent progress in theoretical and experimental studies has clarified many properties of glass transitions [1,2]. However, the mechanism of the glass transition has not yet been fully understood [3]. The major issue is the experimental approach to the investigation of the length scale of the glass transition and dynamics of the α process such as dynamical heterogeneity [4,5]. According to the Adam and Gibbs theory, the dynamics of glass transitions are associated with cooperative motions that are characterized by a so-called *cooperatively rearranging region* (CRR), in which molecules move cooperatively with each other [6]. The size of the CRR is assumed to increase as temperature decreases to the glass transition temperature T_g. The characteristic length scale associated with such cooperative motions has been investigated by multidimensional NMR [7], dielectric hole burning [8], and photobleaching [9] for bulk systems. Another approach to studying the length scale is the investigation of the finite-size effect on glass transition dynamics through confined systems such as thin polymer films [10] or small molecules in nanopores [11].

The first direct measurement of the reduction in T_g in thin polymer films has been made by Keddie *et al.* in 1994 [12]. In their work, the film thickness of the thin films of polystyrene (PS) supported on a hydrogen passivated silicon wafer has been measured as a function of temperature by an ellipsometer. The results showed that the observed T_g in such thin films can be described as a function of film thickness, d, as follows:

$$T_\mathrm{g}(d) = T_\mathrm{g}^\infty \left[1 - \left(\frac{A}{d} \right)^\delta \right], \tag{1}$$

where the best-fit parameters are $T_\mathrm{g}^\infty = 373.8$ K, $A = 1.3 \pm 0.1$ nm, and $\delta = 1.28 \pm 0.20$ [13]. The molecular weight (M_w) dependence of $T_\mathrm{g}(d)$ has not been observed for M_w range from 1.2×10^5 to 2.9×10^6, and hence, it was concluded that the confinement effect of polymer chains within thin layers may be neglected in such systems. Further measurements of T_g in thin films of poly(methyl methacrylate) (PMMA) supported on two different kinds of substrate revealed that the strong attractive interactions between substrate and polymers lead to increase in T_g with decreasing film thickness [14].

In order to remove such interactions between substrate and polymers, Forrest *et al.* measured T_g for *freely standing films* of polystyrene by Brillouin light-scattering measurements [15,16]. They obtained the thickness dependence of T_g as follows:

$$T_\mathrm{g}(d) = \begin{cases} T_\mathrm{g}^\infty \left(1 - \dfrac{d_0 - d}{\zeta} \right) & : \quad d < d_0 \\ T_\mathrm{g}^\infty & : \quad d > d_0, \end{cases} \tag{2}$$

where T_g^∞ is the glass transition temperature for thick films, ζ is the constant, and d_0 is the critical thickness. The critical thickness d_0, below which T_g decreases linearly with decreasing film thickness, depends on the molecular weight, i.e., d_0 increases with the molecular weight in a way similar to the radius of gyration of polymer chains.

In our previous papers, we performed electric capacitance measurements for thin films of polystyrene supported on Al-deposited glass substrate and determined the T_g as a temperature at which the temperature dependence of capacitance changes discontinuously [17,18]. As a result, we confirmed the reduction of T_g in our system in a way similar to Eq. (1).

---

[*] Author to whom correspondence should be addressed. Present address: Department of Polymer Science and Engineering, Kyoto Institute of Technology, Matsugasaki, Sakyo-ku, Kyoto 606-8585, Japan. Electronic address: fukao@ipc.kit.ac.jp

TABLE I. The weight averaged molecular weight M_w, the ratio of M_w to the number averaged molecular weight M_n, and radius of gyration of the polymers R_g used in these studies.

	M_w	M_w/M_n	R_g(nm)[a]
PVAc	124800	2.37	10.1
	182000	2.95	12.2
	237100	2.64	12.8
PMMA	490200	4.11	18.6

[a]The values of R_g are obtained from Ref. [22].

Furthermore, we made volume relaxation measurements on thin polystyrene films and measured the temperature T_α at which the imaginary component of complex thermal-expansion coefficient has a peak at a given very low frequency corresponding to the relaxation time about 100 sec during the heating process of a constant rate [19,20]. The temperature T_α thereby obtained may be regarded as the glass transition temperature T_g. In our measurements, it is found that T_g decreases slightly with decreasing film thickness down to a critical thickness d_c, and below d_c it decreases very rapidly. The value of d_c changes with M_w in the similar way to the radius of gyration of polymer chains. This behavior of T_g is quite similar to those obtained in freely standing films as shown in Eq. (2) except the slight change in T_g above d_c.

Intensive investigations have been performed so far mainly on polystyrene films [10]. It is important to clarify whether the results extracted from the investigations on thin polystyrene films hold also for other polymers. In this paper, therefore, we investigate the dynamics of thin films of poly(vinyl acetate)(PVAc) and PMMA by dielectric relaxation spectroscopy. PVAc is a polymer suitable for dielectric relaxation measurements because a monomer unit of PVAc has a large dipole moment [21]. In PMMA, there is a strong β process that is due to the hindered rotation of the side group in addition to the α process [21]. It is indispensable to investigate the size dependence of dynamics of the α process and the β process when elucidating the nature of glass transition.

This paper consists of five sections. After the introduction, experimental details on preparation method of thin films and dielectric relaxation spectroscopy are given in Sec. II. In Sec. III, experimental results on poly(vinyl acetate) and poly(methyl methacrylate) by dielectric relaxation spectroscopy are shown. In particular, thickness dependence of the temperatures T_α and T_β corresponding to the α and β peaks in the dielectric loss and the width of the distribution of the relaxation time of the α and β processes are focused in Sec. III. Discussions on the present experimental results compared with the results reported previously are given in Sec. IV and a summary is given in Sec. V.

II. EXPERIMENTS

The polymer samples used in this study (PVAc and PMMA) are purchased from Scientific Polymer Products, Inc. The molecular weight and radius of gyration of the polymers are listed in Table I. The glass transition temperatures of PVAc and PMMA in the bulk states are 303 and 373 K, respectively. Thin polymer films were prepared by spin coating a toluene solution of PVAc (PMMA) onto Al-deposited glass substrate. Film thickness is controlled by changing the concentration of the solution. The thin films obtained by the spin-coat method were annealed *in vacuo* for 48 hours at 303 K for PVAc and 353 K for PMMA, respectively. After annealing, Al was vacuum deposited once more onto the thin films to serve an upper electrode. Vacuum deposition of Al might increase the temperature of thin polymer films locally. However, no dewetting of polymer films has been observed during the vacuum deposition of Al. Therefore, the local heating of thin polymer films by the vacuum deposition, if any, would not affect the present experimental results.

Dielectric measurements were performed by using an LCR meter (HP4284A) for the frequency range from 20 Hz to 1 MHz and an impedance analyzer (Solartron Instruments SI1260) for the frequency range from 0.1 Hz to 1 MHz. The temperature of a sample cell was changed between 273 and 373 K for PVAc and between 263 and 423 K for PMMA at a constant rate of 0.5 K/min. The dielectric measurements during the heating and cooling processes were performed repeatedly several times. Data acquisition was made during the above cycles except the first cycle. The good reproducibility of dielectric data was obtained after the first cycle.

The thickness d is related to the electric capacitance C' of thin films in the following way: $C'=\epsilon'\epsilon_0(S/d)$, where ϵ_0 is the permittivity of the vacuum, ϵ' is the permittivity of the polymer (PVAc or PMMA), and S is the effective area of the electrode ($S=8.0\ \text{mm}^2$). For the frequency range where there are no contributions due to any dielectric dispersion, ϵ' may be regarded as constant for any change in frequency, and hence, the film thickness is inversely proportional to the electric capacitance. Relative film thickness at a given temperature may be obtained from the electric capacitance of the thin films at a frequency within the above-frequency range. The frequency and the temperature we chose for the determination of the relative thickness are 8 kHz and 298 K for PVAc, and 1 kHz and 273 K for PMMA. The absolute values of the film thickness for several films were measured directly by an atomic force microscope (Shimadzu SPM-9500) in order to calibrate the film thickness.

As shown in a previous paper [18], the resistance of the Al electrodes cannot be neglected for dielectric measurements of very thin films. This resistance leads to an artifact loss peak on the high-frequency side; this peak results from the fact that the system is equivalent to a series circuit of a capacitor and resistor [23]. Because the peak shape in the frequency domain is described by a Debye-type equation, the ''C-R peak'' can easily be subtracted. The data thus corrected were used for further analysis in the frequency domain.

III. RESULTS

A. Poly(vinyl acetate)

1. Dielectric relaxation of the α process in PVAc

Figure 1 shows the dependence of the complex electric capacitance ($C^*=C'-iC''$) on the logarithm of frequency

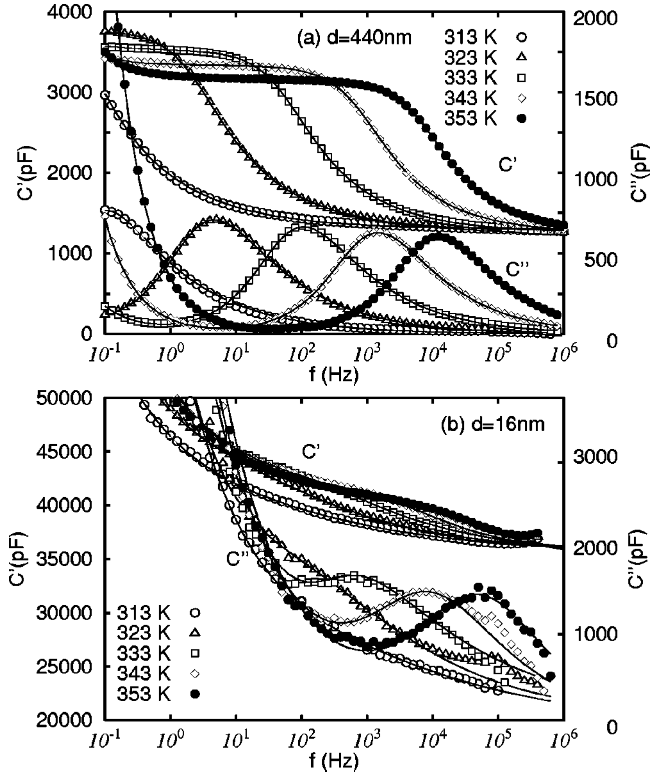

FIG. 1. The dependence of the complex electric capacitance on the logarithm of frequency at various temperatures for PVAc with $M_w = 1.8\times 10^5$: (a) $d = 440$ nm, (b) $d = 16$ nm. Solid curves are calculated by Eq. (3).

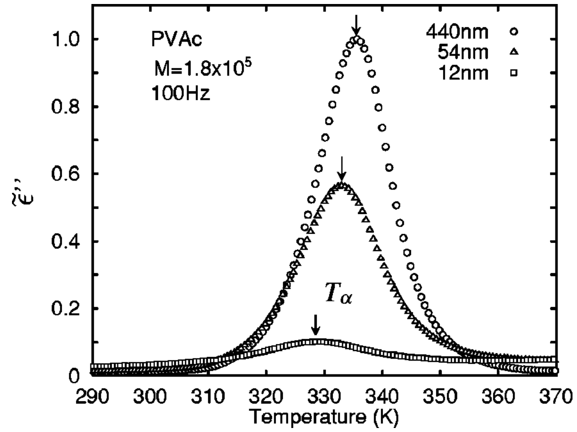

FIG. 2. The temperature dependence of the imaginary part of the complex dielectric constant at 100 Hz for PVAc with $M_w = 1.8\times 10^5$ and three different thicknesses: ○ corresponds to 440 nm, △ to 54 nm, and □ to 12 nm. The value of the vertical axis is normalized with the maximum value for the bulk sample. The arrows indicate the values of T_α at 100 Hz.

at various temperatures for thin films of PVAc with $M_w = 1.8\times 10^5$ and film thicknesses (a) $d = 440$ nm and (b) $d = 16$ nm. In this figure, we find that the imaginary component C'' has a peak due to the α process. The peak frequency shifts to the higher-frequency side as temperature increases. Comparing Figs. 1(a) and 1(b), we find that the peak position shifts to the higher-frequency side at a fixed temperature as the film thickness decreases from 440 to 16 nm.

The temperature change in the dielectric loss at 100 Hz normalized with the peak value for the bulk sample is shown in Fig. 2 in the case of PVAc with $M_w = 1.8\times 10^5$. The dielectric peak due to the α process possesses a maximum at the temperature T_α. It is found in Fig. 2 that the temperature T_α decreases with decreasing film thickness. At the same time, the peak width of the α process increases and the height at T_α decreases with decreasing film thickness. This behavior is related to the change in the distribution of the relaxation times and the relaxation strength with the film thickness.

Figure 3 displays the temperature dependence of the frequency f of the α process for thin films of PVAc with three different thicknesses 440, 62, and 18 nm, where f is associated with a characteristic time of the α process τ_α via the relation $2\pi f\tau_\alpha = 1$. Each point in Fig. 3 consists of a data set $(1/T_\alpha, \log_{10} f)$. For each film thickness, the temperature dependence of τ_α can well be reproduced by the Vogel-Fulcher-Tammann (VFT) law [24]: $\tau_\alpha(T) = \tau_\alpha^\infty \exp[U/(T - T_0)]$, where τ_α^∞ is the relaxation time at very high temperatures, U is the apparent activation energy, and T_0 is the Vogel temperature. At a given temperature, the frequency f increases with decreasing film thickness, i.e., the relaxation becomes faster in thinner films. This thickness dependence of f (and τ_α) becomes stronger as the temperature approaches the glass transition temperature. This behavior is quite similar to that observed in thin films of PS supported on glass substrate [17,18].

In order to check how the α process changes with film thickness, the thickness dependence of the temperature T_α at the frequency 100 Hz is shown in Fig. 4 for three different molecular weights 1.2×10^5, 1.8×10^5, and 2.4×10^5. The error bars in Fig. 4 stand for the standard deviation in T_α for the data acquired by measurements done repeatedly several times. Because the glass transition temperature T_g can be

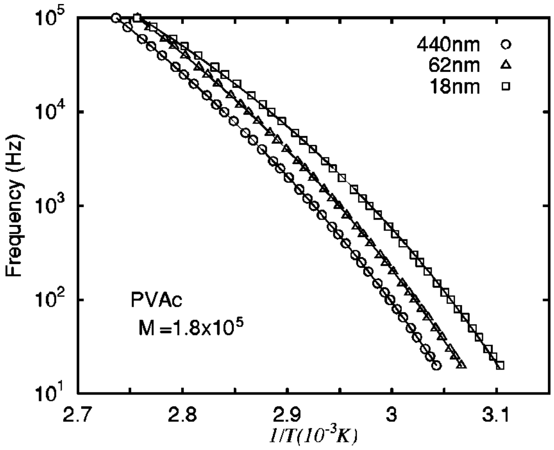

FIG. 3. The relationship between the temperature T_α and the frequency f at which the dielectric loss possesses a maximum due to the α process for PVAc with $M_w = 1.8\times 10^5$ and three different thicknesses: ○ corresponds to 440 nm, △ to 62 nm, and □ to 18 nm. Solid curves are obtained by fitting the data to the VFT equation.

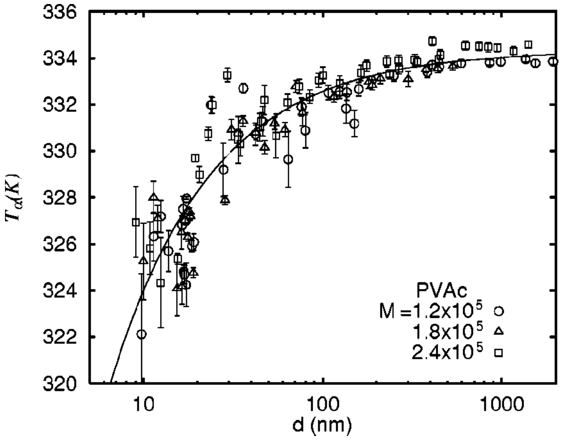

FIG. 4. Thickness dependence of the temperature T_α for PVAc with three different molecular weights: ○ corresponds to $M_{\mathrm{w}}=1.2\times 10^5$, △ to 1.8×10^5, and □ to 2.4×10^5. The temperature T_α is a temperature at which the imaginary component of the complex dielectric constant possesses a maximum value at 100 Hz.

regarded as the value of T_α obtained for a very low frequency of the applied electric field, for example, $f\approx 1/(2\pi\times 10^2\ \mathrm{sec})$, the absolute value of T_{g} is lower than that of the T_α for $f=100$ Hz. However, it is possible to extract qualitative information on the thickness dependence of T_{g} from the observed thickness dependence of T_α in Fig. 4.

The solid curve in Fig. 4 is obtained by using the same form of Eq. (1) in which T_{g} is replaced by T_α with parameters as follows: $T_\alpha^\infty=334.3\pm 0.1$ K, $A=0.11\pm 0.03$ nm, $\delta=0.77\pm 0.04$. Because the single curve can reproduce the observed values of T_α for the three different molecular weights, the temperature T_α seems to have almost no M_{w} dependence, and hence, we conjecture that T_{g} is also independent of the molecular weight for $M_{\mathrm{w}}=1.2\times 10^5$-$2.4\times 10^5$ and $d>10$ nm.

In order to discuss the dynamics of the α process in thin films of PVAc, the observed complex dielectric constant $\epsilon^*(\omega)$ in Fig. 1 is fitted to the following model function:

$$\epsilon^*(\omega)=\epsilon_\infty+A\omega^{-m}e^{-i(\pi/2)m}+\frac{\Delta\epsilon}{[1+(i\omega\tau_0)^{\alpha_{\mathrm{HN}}}]^{\beta_{\mathrm{HN}}}}, \quad (3)$$

where $\omega=2\pi f$ and ϵ_∞ is the permittivity at a very high frequency. The second term in the right-hand side (rhs) is a contribution from space charge [25], and it may be attributed to pure dc conductivity if $m=1$. In the case of PVAc, the fitted value of m was found to be between 0.40 and 0.93 depending on film thickness. The third term in the rhs comes from the α process and its form is empirically proposed by Havriliak-Negami (HN) [26], where $\Delta\epsilon$ is the relaxation strength, τ_0 is the characteristic time, α_{HN} and β_{HN} are the shape parameters.

The thickness dependence of the relaxation strength $\Delta\epsilon$ obtained from the observed values of $\epsilon^*(\omega)$ at 333 K is shown in Fig. 5 for thin films of PVAc with $M_{\mathrm{w}}=2.4\times 10^5$, where $\Delta\epsilon$ is normalized with respect to the value of $\Delta\epsilon$ for the bulk sample (see open circles). The temperature 333 K was chosen because the dielectric loss peak of the α process is located at the center of the frequency window in the present measurement at this temperature. As the film thickness decreases, the normalized relaxation strength decreases from 1 to about 0.2. This behavior in relaxation strength corresponds to the decrease in the height at T_α in dielectric loss in Fig. 2. The d dependence of $\Delta\epsilon$ will be discussed later. The fitting parameters α_{HN} and β_{HN} of the HN equation are shown in Fig. 6. It is found that with decreasing film thickness the parameter α_{HN} decreases and β_{HN} slightly increases. The decrease in α_{HN} with decreasing film thickness implies the broadening of the distribution of the relaxation times.

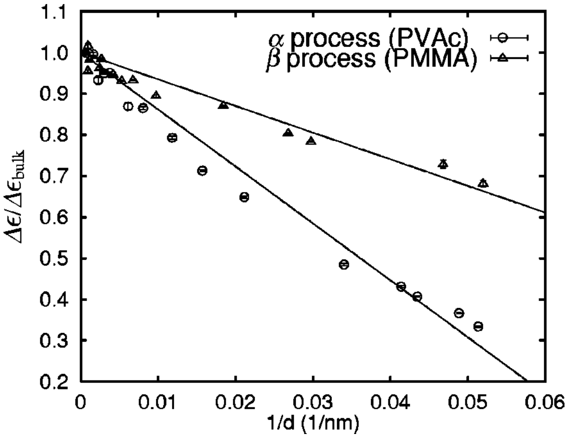

FIG. 5. Thickness dependence of the relaxation strength normalized with the value of the bulk sample. Open circles correspond to the result obtained at 333 K for the α process in PVAc with $M_{\mathrm{w}}=2.4\times 10^5$ and open triangles to the result obtained at temperatures at which the dielectric loss peak is located at 300 Hz for the β process in PMMA with $M_{\mathrm{w}}=4.9\times 10^5$. Solid lines are obtained by Eq. (6). The characteristic lengths are 13.84 ± 0.34 nm and 6.48 ± 0.31 nm for the α process in PVAc and the β process in PMMA, respectively

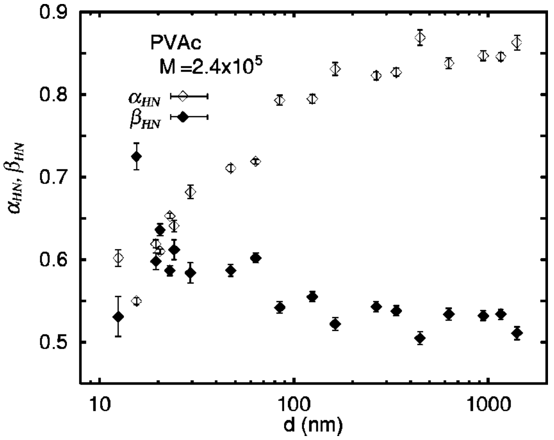

FIG. 6. The thickness dependecne of the shape parameters α_{HN} and β_{HN} of the HN equation obtained by fitting the observed data at 333 K for PVAc with $M_{\mathrm{w}}=2.4\times 10^5$: open diamonds correspond to α_{HN} and full diamonds to β_{HN}.

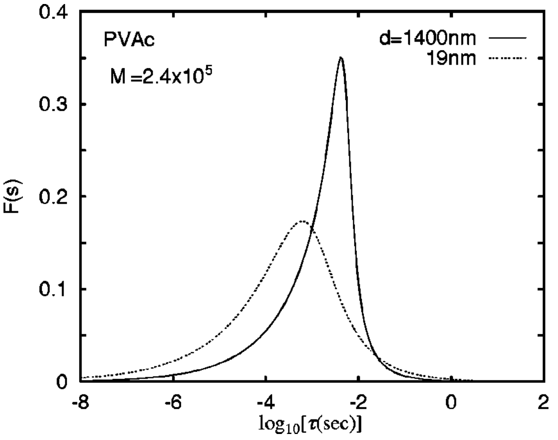

FIG. 7. The distribution function $F(s)$ of the relaxation times of the α process at 333 K for PVAc with $M_w = 2.4\times10^5$. The values are calculated by Eq. (5) with the best-fit parameters of the HN equation. The solid curve stands for the result of $d = 1400$ nm and the dotted curve for that of $d = 19$ nm.

2. Distribution of the relaxation times

The experimental observation that the $\epsilon^*(\omega)$ does not obey a simple Debye equation but rather a complicated HN equation may be accounted for by assuming that $\epsilon^*(\omega)$ is expressed as the sum of the Debye equations with different relaxation times in the following way:

$$\epsilon^*(\omega) = \epsilon_\infty + \Delta\epsilon \int_{-\infty}^{+\infty} \frac{F(\log_e \tau)\, d(\log_e \tau)}{1 + i\omega\tau}, \tag{4}$$

where the second term in Eq. (3) is omitted. $F(s)$ is a distribution function of the logarithm of the relaxation times of the α process ($s = \log_e \tau$) and is normalized as follows: $\int_{-\infty}^{+\infty} F(s)\, ds = 1$. If it is assumed that $\epsilon^*(\omega)$ is expressed by the HN equation, the analytical form of $F(s)$ may easily be obtained in the following way with the parameters α_{HN}, β_{HN}, and τ_0:

$$F(s) = \frac{1}{\pi}\left[1 + 2e^{\alpha_{\mathrm{HN}}(x_0 - s)} \sin \pi\alpha_{\mathrm{HN}} + e^{2\alpha_{\mathrm{HN}}(x_0 - s)}\right]^{-\beta_{\mathrm{HN}}/2} \times \sin\left[\beta_{\mathrm{HN}} \tan^{-1}\left(\frac{e^{\alpha_{\mathrm{HN}}(x_0 - s)} \sin \pi\alpha_{\mathrm{HN}}}{1 + e^{\alpha_{\mathrm{HN}}(x_0 - s)} \cos \pi\alpha_{\mathrm{HN}}}\right)\right], \tag{5}$$

where $x_0 = \log_e \tau_0$.

Figure 7 displays the distribution of $\log_{10} \tau_\alpha$ calculated in terms of Eq. (5) with the parameters α_{HN}, β_{HN}, and τ_0 at 333 K for thin films of PVAc with $M_w = 2.4\times10^5$ and $d = 1400$ and 19 nm. In this figure, it is found that the average relaxation time of the α process decreases with decreasing film thickness, and that the width of the distribution of the relaxation times τ_α becomes broader in thinner films. In order to quantify the change in the distribution of τ_α, the full width w at the half maximum (FWHM w) at 333 K of $F(s)$ was evaluated as shown in Fig. 8(a) for thin films of PVAc with $M_w = 2.4\times10^5$ (see open circles). It is found that the width w increases with decreasing film thickness. The thickness dependence of w is given by the equation $w(d) = w_0(1 + a/d)$, where $w_0 = 0.92 \pm 0.03$ and $a = 22.0 \pm 1.6$ nm for the α process of PVAc. This broadening of the distribution of the relaxation times and its functional form have also been observed in thin films of polystyrene by dielectric relaxation spectroscopy [18] and ellipsometric measurements [27].

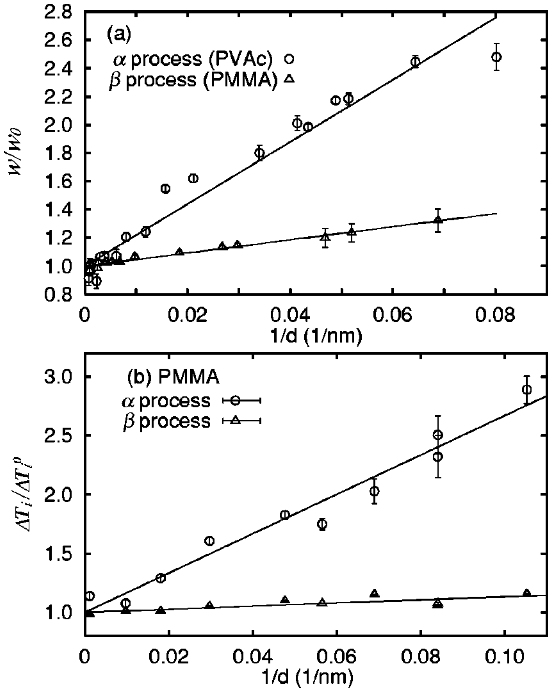

FIG. 8. (a) The thickness dependence of the normalized full width at the half maximum w/w_0 for the α process in PVAc with $M_w = 2.4\times10^5$ (○), and the β in PMMA with $M_w = 4.9\times10^5$ (△). The width for PVAc is evaluated at 333 K and that for PMMA is at the temperature at which the β peak in the dielectric loss is located at 300 Hz. (b) The thickness dependence of the width ΔT_α and ΔT_β of the α, β peaks in the dielectric loss at 40 Hz in the temperature domain. The width is normalized with that of the bulk sample.

B. Poly(methyl methacrylate)

1. Temperature dispersion of dielectric loss

Figure 9 shows the temperature change in the imaginary part of the complex dielectric constant at a fixed frequency for PMMA with $M_w = 4.9\times10^5$ and $d = 900$ and 9.5 nm. The value of $\tilde{\epsilon}''$ is normalized with the maximum value for the bulk sample ($d = 900$ nm). The value $\tilde{\epsilon}''$ at a fixed frequency (40 Hz) displays an anomalous increase with temperature due to the α and β processes, and it possesses two maxima at the temperatures T_α and T_β. The values of T_α and T_β depend not only on the frequency f but also on the film thickness, as we may see in Fig. 9; in the case of $f = 40$ Hz, $T_\alpha = 401$ K and $T_\beta = 320$ K for $d = 900$ nm, and $T_\alpha = 383$ K and $T_\beta = 301$ K for $d = 9.5$ nm. Both the height and the width of the β peak are larger than those of the α peak. The origin of the α process is attributed to the micro-

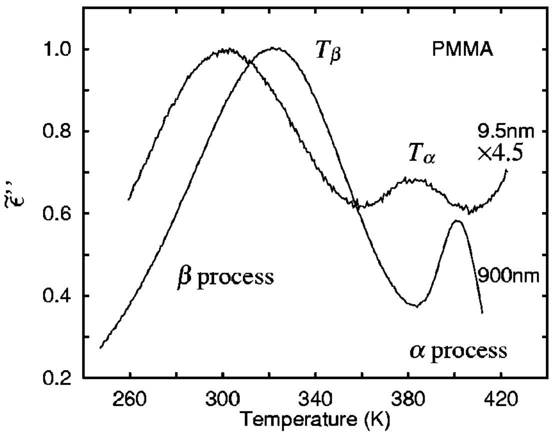

FIG. 9. The temperature dependence of the imaginary part of the complex dielectric constant at 40 Hz for PMMA with the thickness of 9.5 and 900 nm. The vertical axis is normalized with the maximum value for the bulk sample. The value for $d = 9.5$ nm is magnified by a factor of 4.5.

Brownian motion of the polymer main chain, while that of the β process is to the hindered rotation of the side branch of PMMA [21].

In order to extract the peak temperatures T_α and T_β and the widths ΔT_α and ΔT_β, the observed values ϵ'' as a function of temperature were fitted by the sum of the two Lorentzian functions $\tilde{\epsilon}_i''/\{1+[(T-T_i)/\Delta T_i]^2\}$ $(i=\alpha,\beta)$. The functional form has no physical meaning, but it is used only to obtain the peak temperature and the width. If necessary, the contribution due to dc conductivity was also taken into account by adding another peak at higher temperature to the fitting function. The thickness dependence of the widths of the α and β processes in the temperature domain, normalized with those in the bulk sample $\Delta T_i/\Delta T_i^0$ is shown in Fig. 8(b), where ΔT_i^0 is the width for the bulk sample. The solid lines in Fig. 8(b) are given by $\Delta T_i(d) = \Delta T_i^0(1+a/d)$. In PMMA, $\Delta T_\alpha^0 = 7.9 \pm 0.5$ K and $a = 16.7 \pm 2.0$ nm for the α process and $\Delta T_\beta^0 = 48.4 \pm 0.9$ K and $a = 1.3 \pm 0.3$ nm for the β process.

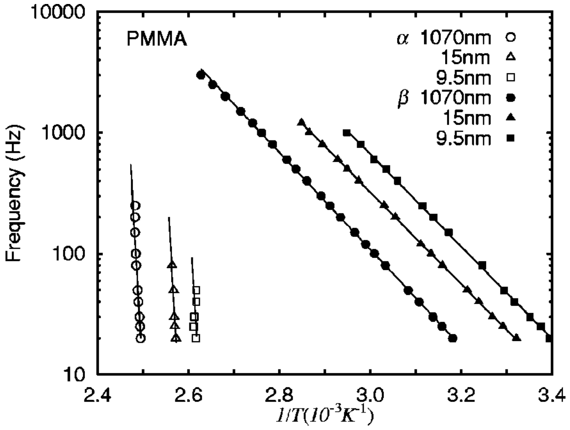

FIG. 10. Dispersion map of PMMA for various thicknesses. Circles correspond to $d = 1070$ nm, triangles to $d = 15$ nm, and boxes to $d = 9.5$ nm. Full and open symbols are for the α process and the β process, respectively.

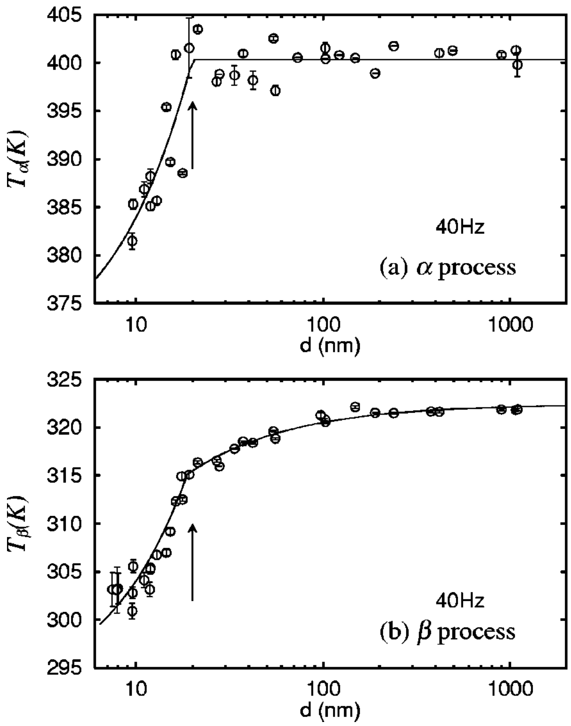

FIG. 11. Thickness dependence of T_α and T_β at 40 Hz for PMMA. The arrows indicate the critical thickness d_c.

The dependence of the frequency f on the reciprocal of the temperatures T_α and T_β is shown in the dispersion map of Fig. 10 for PMMA with $M_w = 4.9 \times 10^5$ with three different film thicknesses. The number of data points of the α process is limited because the small α peak merges with the large β peak as the frequency increases, and as a result it is much more difficult to extract T_α at higher frequencies.

As shown in Fig. 10, the branch of the β process is well separated from that of the α process for the frequency range below about 500 Hz. However, the β process approaches the α process as the frequency or the temperature increases, because the slope of the straight line corresponding to the β process is much smaller than that of the α process: the corresponding apparent activation energies in this frequency range are 651 ± 6 kJ/mol for the α process and 32.7 ± 0.2 kJ/mol for the β process. In this limited frequency range investigated here, thickness dependence of the apparent activation energy cannot be observed. (Here, it should be noted that the α branch may indeed be fitted by a straight line in Fig. 10, because of the limitation of the frequency range, but we do not intend to deny the validity of the VFT law.) In Fig. 10, we find that both the α and β processes shift to the higher-frequency side at a fixed temperature, as the thickness decreases, i.e., both the relaxations become faster.

2. T_α and T_β as a function of thickness

In order to quantify the thickness dependence of T_α and T_β, the frequency is fixed to be 40 Hz and the temperatures T_α and T_β are evaluated from the observed curve of ϵ'' vs T for various film thicknesses from 9.5 to 1000 nm. The results are summarized in Fig. 11, where Figs. 11(a) and 11(b) dis-

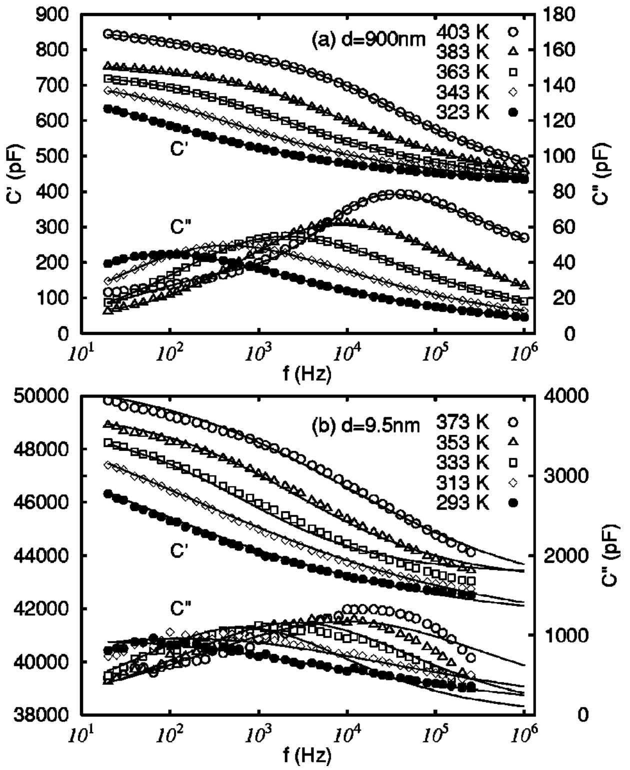

FIG. 12. The dependence of the complex electric capacitance on the logarithm of frequency at various temperatures for PMMA with $M_w = 4.9\times10^5$: (a) $d = 900$ nm, (b) $d = 9.5$ nm. Solid curves are calculated by the sum of two HN equations.

play the thickness dependence of the temperatures T_α and T_β observed at 40 Hz for the thin films of PMMA with $M_w = 4.9\times10^5$, respectively.

Figure 11(a) shows that T_α *remains almost constant* within the experimental accuracy as the film thickness decreases down to a critical thickness $d_{\alpha,c}$, at which point T_α begins to decrease rapidly with d. The solid curve in Fig. 11(a) below $d_{\alpha,c}$ is given by a linear relation between T_α and d, although it does not appear to be a straight line because of the logarithmic scale of the horizontal axis. The amount of the depression of T_α in the thin films is about 20 K between the bulk sample and the thinnest film with $d = 9.5$ nm. In this case, the critical thickness $d_{\alpha,c}$ is found to be about 20 nm for the α process at 40 Hz.

On the other hand, thickness dependence of T_β seems to be to some extent different from that of T_α, as shown in Fig. 11(b). The temperature T_β *decreases slightly with decreasing film thickness* down to a critical thickness $d_{\beta,c}$ even for the relatively thick films. Below a critical thickness $d_{\beta,c}$, T_β decreases more rapidly with decreasing film thickness. The depression in T_β is about 25 K also in this case for the thickness range investigated here, and the critical thickness $d_{\beta,c}$ is about 19 nm. It is quite interesting that the critical thickness of the β process almost agrees with that of the α process; $d_{\alpha,c} \approx d_{\beta,c} (\equiv d_c)$. This result may suggest that there is a strong correlation between the α process and the β process, although the two processes at 40 Hz exist quite separately on the dispersion map in Fig. 10.

In order to investigate the dynamical behavior in thin films of PMMA with $d = 900$ and 9.5 nm, we observed the frequency dependence of the complex dielectric constant at a fixed temperature, as shown in Fig. 12. Corresponding to Fig. 9, the large peak due to the β process may be seen in the C'' vs f plot and a small contribution from the α process may also be observed at the foot of the large β peak at 403 K. According to the procedure of data analysis done for PVAc, the observed C^* is fitted to a model function consisting of the two HN functions. In Fig. 12, the calculated values with this model function are shown as solid curves. For thick films, the model function may very well reproduce the observed results for the temperature and frequency range shown in Fig. 12. For very thin films, the data at higher frequency (above 10^4 Hz) include relatively large errors. Therefore, in such a case, we used the data below 10^4 Hz for the data fitting.

In order to evaluate the distribution $F(s)$ and the relaxation strength $\Delta\epsilon$, the fitting parameters were obtained for the β process at the temperature at which the β peak is located at 300 Hz for various film thicknesses. In this case, because the temperatures are located between 323 and 338 K depending on the film thickness, the contribution from the α process can safely be neglected. Using the parameters $\alpha_{\mathrm{HN},\beta}$, $\beta_{\mathrm{HN},\beta}$, and $\tau_{0,\beta}$ obtained by fitting to the HN equation, we evaluated the distribution function $F(s)$ of the relaxation time of the β process for PMMA, where the subscript β means that these parameters are obtained for the β process, and then we obtained the thickness dependence of FWHM w. The result of w is shown in Fig. 8(a) (see open triangles). For the β process of PMMA, $w_0 = 4.7 \pm 0.2$ and $a = 3.20 \pm 0.02$ nm. In this figure, the result of w for the α process in PVAc is also shown instead of w for the α process in PMMA, because it was difficult to obtain w for the α process in PMMA. In addition to w, the normalized widths of the dielectric loss peak in the temperature domain due to the α and β processes, $\Delta T_i / \Delta T_i^0$ $(i = \alpha, \beta)$, are also shown in Fig. 8(b). Because the relaxation time τ is a function of the temperature T, the distribution function of relaxation times $F(\log_e \tau)$ may be converted into that in the temperature domain, where the distribution function of the relaxation times with respect to temperature is given by $\tilde{F}(T) \equiv F[\log_e \tau(T)](d \log_e \tau/dT)$. Therefore, the distribution of the relaxation time can be evaluated not only from $F(\log_e \tau)$ but also from the width in the temperature domain. Comparing these results with each other, we found that the distribution of the relaxation times of the α process becomes much broader with decreasing film thickness, while for the β process, this broadening is weaker or remains almost constant with decreasing film thickness.

Figure 5 shows the dependence of normalized relaxation strength on the reciprocal of film thickness for the β process in thin films of PMMA (see open triangles). The relaxation strengths are obtained by fitting the observed frequency dependence of dielectric loss for the β process at temperature at which the β peaks are located at 300 Hz. The dependence of normalized relaxation strength of the α process in thin films of PVAc with $M_w = 2.4\times10^5$ is also shown in Fig. 5.

However, that of the α process in PMMA has not yet been evaluated because the dielectric loss due to the α process in this case is much smaller than that due to the β process. More precise and wider frequency range measurements will be required to extract the relaxation strength of the α process in PMMA especially in thinner films.

In Fig. 5, it is found that the dielectric strengths of both the processes have a similar thickness dependence as follows:

$$\Delta\epsilon/\Delta\epsilon_{bulk}=1-\frac{\tilde{a}}{d}, \tag{6}$$

where $\Delta\epsilon_{bulk}$ is the relaxation strength of the bulk sample, and $\tilde{a}$ is a constant independent of d. The characteristic lengths fitted by Eq. (6) are 13.8 ± 0.3 and 6.5 ± 0.3 nm for the α process in PVAc and the β process in PMMA, respectively.

IV. DISCUSSIONS

We have successfully observed many properties of dynamics of the α process in PVAc and the α and β processes in PMMA. Here, we will discuss some of the results observed in this study.

A. Thickness dependence of T_α in PVAc

In the case of PVAc, it has been observed that the temperature T_α of the α peak in the temperature domain at 100 Hz decreases with decreasing film thickness in a manner described by Eq. (1). The thickness dependence of T_α has almost no $M_{\rm w}$ dependence in the $M_{\rm w}$ range from 1.2×10^5 to 2.4×10^5.

In the case of the freely standing films of polystyrene, Mattsson *et al.* show that in a low $M_{\rm w}$ regime ($M_{\rm w}\leqslant3.47\times10^5$) the value of $T_{\rm g}$ observed by Brillouin light scattering has no molecular weight dependence and it decreases gradually with decreasing film thickness in a similar way to Eq. (1) [28]. On the other hand, in a high $M_{\rm w}$ regime ($M_{\rm w}\geqslant5.14\times10^5$) the thickness dependence of $T_{\rm g}$ shows a distinct molecular weight dependence given by Eq. (2) and it depends on the radius of gyration of the polymer chain [28].

Although the existence of the interfacial interaction may lead to the difference in the d and $M_{\rm w}$ dependence of $T_{\rm g}$ between the freely standing films and the thin films supported on substrate, our recent study shows that the temperature T_α observed at 100 and 1 kHz by dielectric relaxation spectroscopy has a similar thickness and $M_{\rm w}$ dependence to Eq. (2) for thin PS films supported on Al-deposited glass substrate [17,18]. Therefore, it is expected that the thickness and $M_{\rm w}$ dependence of T_α in thin films supported on substrate may be compared with that of $T_{\rm g}$ in freely standing thin films. For this reason, the observed results on T_α in thin films of PVAc may correspond to the low $M_{\rm w}$ regime observed by Mattsson *et al.* in the freely standing films of PS. In the regime, *confinement effect of polymer chains* within thin films is not dominant for the reduction of $T_{\rm g}$ or T_α, but *the finite-size effects* due to a length scale intrinsic to the glass transition may be dominant. If we measure T_α for thin films of PVAc with still higher molecular weights, however, $M_{\rm w}$ dependence of T_α vs d may be observed in a similar way to $T_{\rm g}$ in the freely standing films of PS.

B. Thickness dependence of T_α and T_β in PMMA

In PMMA, it can be expected that the characteristic length scale of the β process, if any, should be smaller than that of the α process, because the characteristic time of the β process at a fixed temperature in the temperature range investigated here is much shorter than that of the α process. In this case, the thickness dependence of T_α should be stronger than that of T_β at a fixed frequency. However, the observed results do not obey this expectation; as shown in Fig. 11, for $d>d_{\alpha,c}$ ($\approx d_{\beta,c}$), T_α remains *almost independent of thickness* and T_β *decreases slightly with decreasing film thickness*.

According to a layer model, as discussed in the literature [12,18,29], $T_{\rm g}$ and the dynamics of thin films are controlled by the competition between the two different effects. Firstly, the existence of a mobile layer near surfaces leads to the speedup of the dynamics of the α process (and also the β process). Within the mobile layer molecular motions are enhanced compared with those in the bulk state. The origin of the enhancement of molecular motion is supposed to be due to the higher density of chain ends of polymer chains [30] or to the restriction on cooperative motions characteristic of the glass transition within the surface layer [28,31]. In the latter case, the layer thickness of the mobile layer is of an order of the size of the cooperatively rearranging region (CRR) [28]. Secondly, the attractive interaction between the polymers and the substrate leads to the slowing down of the dynamics of the motion [32,33]. For example, the adsorption of polymer chains onto the substrate causes $T_{\rm g}$ of the thin films to increase compared with that in the bulk state.

Here, some comments should be added on the Al electrode of our thin films. In our measurements, the film is covered with Al on both sides. Although the lower Al layer may be regarded as a rigid (solid) wall because of the existence of glass substrate, the upper Al layer cannot be regarded as a rigid wall for the following reasons. (1) After measurements up to about 415 K, ‘‘wrinkles’’ are often observed on the upper Al layer by an optical microscope, which indicates that the upper Al layer is no rigid wall, but it moves according to the thermal expansion of polymer layers. (2) The glass transition temperature of our thin films shows almost same thickness dependence as that of uncapped thin films, which have no upper solid layer but have free surfaces [18]. From these experimental results, it can be expected that the upper Al layer does not affect the thermal properties of polymer films, and accordingly, there may be some mobile layer near the boundary between the upper Al layer and the polymer layer.

In the case of thin films of PMMA, it has been reported that the glass transition temperature strongly depends on the interaction between the polymers and the substrate. Keddie and Jones show that *the* $T_{\rm g}$ *increases with decreasing film thickness* for $\rm SiO_2$ substrate, while *it decreases with decreas-*

ing film thickness for the Au substrate [14]. Local thermal analysis measurements showed that T_g of thin films of PMMA supported on SiO_x is 7 K higher for $d=20$ nm than that for the bulk films, while T_g on SiO_x with hexamethyldisilizane is 10 K lower for $d=20$ nm [34]. In thin films of PMMA supported on Al-deposited silicon substrate, it is reported that T_g of thin films with $d=40$ nm is higher by 14 ± 4 K than that of bulk PMMA [35].

The above results appear to contradict with the present results. However, by comparing the present results with those obtained by other methods, it can easily be found that all results except ours are those for thin films with $d>20$ nm. Our measurements show that for $d>20$ nm, T_α remains almost constant within experimental accuracy, or T_α might increase slightly with decreasing film thickness. If we would measure T_α at much lower frequency than 40 Hz, say, 1 mHz, we could observe more distinct thickness dependence for $d>20$ nm. Therefore, for this thickness range, the present results are not inconsistent with those reported in the literature. The decrease in T_α (T_g) with decreasing film thickness below about 20 nm may also be observed by ellipsometry or local thermal analysis if the measurements will be done for thin films with $d<20$ nm.

In the case of PVAc and PMMA, strong attractive interactions with hydroxyl groups present at aluminum surface are developed. If the Al surface is fixed on glass substrate, this strong attractive interaction may reduce the chain mobility and, as a result, T_g increases with decreasing film thickness. However, it can be expected that, even if there is the attractive interaction between polymers and the *upper* Al layer, this interaction may not contribute to the reduction of chain mobility because the upper Al layer is not fixed with glass substrate and it moves according to the thermal expansion of the polymer layer.

The results reported in the literature [13,34,35] suggest that the effect of the interaction between the polymer and the substrate is sensitive to the condition of the surface of the substrate in thin films of PMMA. In the α process in PMMA on Al-deposited substrate, the mobile layer associated with cooperative length scale of the glass transition tends to reduce T_g and T_α, while the attractive interaction between the polymer and the substrate tends to increase them. As a result, the two effects cancel each other out and the observed value of T_α may *remain almost constant* for $d>d_{\alpha,c}$, as shown in Fig. 11(a). For the β process, it is expected that the two effects no longer cancel each other out and the mobile layer has a dominant effect on T_β. In order to check the validity of the above idea, we should measure T_α and T_β of PMMA thin films for a substrate that has almost no attractive interaction between the polymer and the substrate. In such a case, it is expected that as the thickness decreases, T_α decreases faster than does T_β.

In the present measurements, it is observed that for $d<d_{\alpha,c}$ a drastic decrease in T_α begins with decreasing film thickness. To our surprise, T_β also begins to decrease drastically with decreasing film thickness at almost the same film thickness $d_{\beta,c}(\approx d_{\alpha,c})$. This indicates that there is a strong correlation between the α process and the β process in PMMA thin films, although both processes are located away from each other in the dispersion map (Fig. 10). Both values of $d_{\alpha,c}$ and $d_{\beta,c}$ agree well with the radius of gyration of the polymer chain ($R_g\approx18.6$ nm), and hence, this behavior may be controlled by the polymeric nature of PMMA.

For bulk polymers, the coupling between the α process and β process has been investigated by multidimensional NMR [36] and dielectric relaxation spectroscopy [37,38]. Spiess *et al.* show that in PMMA, the β process predominantly influences the time scale of the α process, leading to a particularly high mobility of the main chain itself. This coupling observed in the bulk PMMA may be related to the correlation between the thickness dependence of T_α and that of T_β. At the moment, it is impossible to answer the question of whether the correlation between these two relaxation processes is stronger in thin PMMA films than in the bulk.

The drastic change at $d_{\alpha,c}$ implies the crossover from the normal α process to other type of dynamics. Recently, de Gennes proposed a sliding motion, which can be activated via a soft skin layer near the surface instead of normal α dynamics [39,40]. Below d_c, the sliding motion may be activated in this case. The measurements of M_w dependence of T_α and T_β for thin films of PMMA are highly desirable in order to clarify the nature of the above behavior on T_α and T_β.

C. Distribution of the relaxation times

The distribution of the relaxation times of the α-process τ_α in thin films of PVAc has been found to become broader with decreasing film thickness. The width w of the distribution in PVAc with $d=9.5$ nm is about 2.5 times as broad as that in bulk PVAc. On the other hand, the width w for the β process in thin films of PMMA depends on film thickness much more weakly, as shown in Fig. 8(a). The corresponding width ΔT_i in temperature domain has a similar thickness dependence, i.e., the thickness dependence of ΔT_β is much weaker than that of ΔT_α in PMMA. From these observations, it is found that the distribution of relaxation times of the α process depends on film thickness much stronger than that of the β process. The intrinsic length scale of the β process is expected to be much smaller than that of the α process, as deduced from Fig. 10. The present observation on the thickness dependence of the distribution of the relaxation times is consistent with this expectation.

D. Thickness dependence of $\Delta\epsilon$

As shown in Fig. 2, the dielectric loss peak due to the α process becomes more depressed with decreasing film thickness. This is consistent with the result that the relaxation strength $\Delta\epsilon$ decreases with decreasing film thickness, as shown in Fig. 5. The thickness dependence of $\Delta\epsilon$ is found to obey Eq. (6). Here, we will try to give a possible explanation on the decrease in $\Delta\epsilon$ with decreasing thickness.

If there is no interaction between dipole moments, the relaxation strength $\Delta\epsilon_0$ is described as follows:

$$\Delta\epsilon_0\approx\frac{N\mu_0^2}{3k_BT}, \tag{7}$$

where N is the dipole number density, μ_0 is the dipole moment of the relaxing unit, k_B is the Boltzmann constant, and T is the temperature. Now it is assumed that *n neighboring dipole moments are relaxed in a cooperative manner*. Then N and μ_0 should be replaced by N/n and $n\mu_0$ in Eq. (7), respectively. As a result, we obtain the relaxation strength $\Delta\epsilon_n$ for such a cooperative motion in the following way:

$$\Delta\epsilon_n \approx n\frac{N\mu_0^2}{3k_B T}. \tag{8}$$

Here, it may be expected that the number n is proportional to the intrinsic length of the motion in question. Because cooperative motions are disturbed near surfaces or interfaces, the intrinsic length of the motions may be reduced and n is decreased. Therefore, $\Delta\epsilon$ of the region near surfaces and interfaces can be expected to be smaller than that of the bulk system. By averaging along the direction normal to the film surface, the relaxation strength $\Delta\epsilon$ is expressed by

$$\Delta\epsilon = \Delta\epsilon_{bulk}\left[1-\xi\left(1-\frac{\Delta\epsilon_{surf}}{\Delta\epsilon_{bulk}}\right)\frac{1}{d}\right], \tag{9}$$

where ξ is the effective thickness of the surface region, d is the overall thickness, and $\Delta\epsilon_{bulk}$ and $\Delta\epsilon_{surf}$ are the relaxation strength of the bulk region and the surface regions, respectively. Here, the relation $\Delta\epsilon_{bulk} > \Delta\epsilon_{surf}$ is satisfied. On the basis of this simple picture, the observed thickness dependence of $\Delta\epsilon$ in Eq. (6) may be reproduced. The value of $\tilde{a}$ is given by $\tilde{a} = \xi(1-\Delta\epsilon_{surf}/\Delta\epsilon_{bulk})$. Therefore, the observed result on $\Delta\epsilon$ in the present measurements is consistent with the idea of cooperative motions.

V. SUMMARY

We made dielectric relaxation measurements for thin films of poly(vinyl acetate) and poly(methyl methacrylate) supported on Al-deposited glass substrate. The results obtained in the present measurements are summarized as follows:

(1) The temperature T_α corresponding to the peak in the dielectric loss due to the α process at 100 Hz is measured as a function of film thickness for thin films of PVAc with three different molecular weights $M_w = 1.2\times10^5$, 1.8×10^5, and 2.4×10^5. It is found that T_α decreases gradually with decreasing film thickness and the decreasing rate of T_α increases more and more in thinner films. Furthermore, T_α has almost no molecular weight dependence.

(2) The width of the distribution of the relaxation times of the α process increases with decreasing film thickness, while the relaxation strength of the α process decreases with decreasing film thickness.

(3) The thickness dependence of the temperatures T_α and T_β corresponding to the peaks in the dielectric loss due to the α and β processes at 40 Hz, respectively, are measured for thin films of PMMA with $M_w = 4.9\times10^5$. The temperature T_α remains almost constant as the thickness is decreased down to a critical thickness $d_{\alpha,c}$, at which point it begins to decrease with thickness. The value of $d_{\alpha,c}$ is about 20 nm. On the other hand, the temperature T_β decreases slightly with decreasing film thickness from the bulk to a critical thickness $d_{\beta,c}$. Below $d_{\beta,c}$, T_β decreases more rapidly with decreasing film thickness. The value of $d_{\beta,c}$ is almost equal to $d_{\alpha,c}$.

(4) The widths ΔT_α and ΔT_β of the peaks in dielectric loss in the temperature domain are measured for both the α and β processes in thin films of PMMA with $M_w = 4.9\times10^5$. As the thickness is decreased, the width ΔT_α increases much faster than ΔT_β. This indicates that the broadening of the distribution of relaxation times of the α process is much more sensitive to the change in thickness than that of the β process.

Here, it should be noted that the experimental values of T_g can be defined in two different ways. One is the temperature at which the slope of the straight line of volume vs temperature changes discontinuously and may be observed by ''dilatometry.'' The other is the temperature at which the characteristic time of the α process because 10^2 sec or 10^3 sec observed by relaxation measurements such as dielectric relaxation spectroscopy. The former is called thermodynamic measure of T_g (thermodynamic T_g) and the latter is called dynamic measure of T_g (dynamic T_g). It is not yet clear whether both two T_g's agree with each other. In our previous papers [18,20], it is found that the thermodynamic T_g has no molecular weight dependence, while the dynamic T_g has a distinct molecular weight dependence in the case of thin supported films of polystyrene. It is also found in Ref. [17] that there is a correlation between the d dependence of the thermodynamic T_g and the width of the loss peak due to the α process. In this paper, several properties of the dynamic T_g have been measured and discussed.

In this paper, several length scales characteristic of the thickness change in T_α, ΔT_α, T_β, ΔT_β, $\Delta\epsilon$, and w have been introduced. The physical quantities such as ΔT_α, ΔT_β, w, and $\Delta\epsilon$ have been found to be described by the linear equation of the reciprocal of d. This result suggests that a layer model be applicable to explain the thickness dependence, as shown in Sec. IV D. In such cases, the characteristic lengths a and $\tilde{a}$ are correlated with the thickness of the surface layer ξ, which can be expected to be comparable to the size of the CRR. On the other hand, the crossover thicknesses $d_{\alpha,c}$ and $d_{\beta,c}$ are almost equal to the radius of gyration of the polymer chain and are expected to be molecular weight dependent. These crossover thicknesses may be strongly associated with dynamics of polymer chains. In order to understand the present experimental results, a model will be required, where the nature of polymer dynamics is taken into account, as well as the intrinsic nature of the glass transition.

ACKNOWLEDGMENTS

This work was partly supported by a Grant-in-Aid (No. 11640395) from the Ministry of Education, Science, Sports and Culture of Japan, and a Grant-in-Aid for Scientific Research on Priority Areas, Mechanism of Polymer Crystallization (No. 12127203).

[1] Proceedings of the 3rd International Discussion Meeting on Relaxations in Complex Systems, edited by K.L. Ngai, E. Riande, and G.B. Wright, J. Non-Cryst. Solids **235-237** (1998).

[2] Proceedings of Yukawa International Seminar on Dynamics of Glass Transition and Related Topics, edited by T. Odagaki, Y. Hiwatari, and J. Matsui, Prog. Theor. Phys. Suppl. **126** (1997).

[3] C.A. Angell, K.L. Ngai, G.B. McKenna, P.F. McMillan, and S.W. Martin, J. Appl. Phys. **88**, 3113 (2000).

[4] M.D. Ediger, C.A. Angell, and S.R. Nagel, J. Phys. Chem. **100**, 13 201 (1996).

[5] H. Sillescu, J. Non-Cryst. Solids **243**, 81 (1999).

[6] G. Adam and J.H. Gibbs, J. Chem. Phys. **43**, 139 (1965).

[7] K. Schmidt-Rohr and H.W. Spiess, Phys. Rev. Lett. **66**, 3020 (1991).

[8] B. Schiener, R. Böhmer, A. Loidl, and R.V. Chamberlin, Science **274**, 752 (1996).

[9] M.T. Cicerone and M.D. Ediger, J. Chem. Phys. **103**, 5684 (1995).

[10] J.A. Forrest and R.A.L. Jones, in *Polymer Surfaces, Interfaces, and Thin Films*, edited by A. Karim and S. Kumar (World Scientific, Singapore, 2000).

[11] Proceedings of International Workshop on Dynamics in Confinement, edited by B. Frick, R. Zorn, and H. Büttner, J. Phys. IV France **10** (2000).

[12] J.L. Keddie, R.A.L. Jones, and R.A. Cory, Europhys. Lett. **27**, 59 (1994).

[13] J.L. Keddie and R.A.L. Jones, Isr. J. Chem. **35**, 21 (1995).

[14] J.L. Keddie and R.A.L. Jones, Faraday Discuss. **98**, 219 (1994).

[15] J.A. Forrest, K. Dalnoki-Veress, J.R. Stevens, and J.R. Dutcher, Phys. Rev. Lett. **77**, 2002 (1996).

[16] J.A. Forrest, K. Dalnoki-Veress, and J.R. Dutcher, Phys. Rev. E **56**, 5705 (1997).

[17] K. Fukao and Y. Miyamoto, Europhys. Lett. **46**, 649 (1999).

[18] K. Fukao and Y. Miyamoto, Phys. Rev. E **61**, 1743 (2000).

[19] K. Fukao and Y. Miyamoto, J. Phys. IV **10**, 243 (2000).

[20] K. Fukao and Y. Miyamoto, Phys. Rev. E **64**, 011803 (2001).

[21] N.G. McCrum, B.E. Read, and G. Williams, *Anelastic and Dielectric Effects in Polymeric Solids* (Wiley, London, 1967).

[22] *Physical Properties of Polymers Handbook*, edited by J.E. Mark (AIP Press, Woodbury, NY, 1996), Chap. 24.

[23] G. Blum, F. Kremer, T. Jaworek, and G. Wegner, Adv. Mater. **7**, 1017 (1995).

[24] H. Vogel, Phys. Z. **22**, 645 (1921); G.S. Fulcher, J. Am. Ceram. Soc. **8**, 339 (1925).

[25] Y. Miyamoto, Polymer **25**, 63 (1984).

[26] S. Havriliak and S. Negami, Polymer **8**, 161 (1967).

[27] S. Kawana and R.A.L. Jones, Phys. Rev. E **63**, 021501 (2001).

[28] J. Mattsson, J.A. Forrest, and L. Börjesson, Phys. Rev. E **62**, 5187 (2000).

[29] G.B. DeMaggio, W.E. Frieze, D.W. Gidley, Ming Zhu, H.A. Hristov, and A.F. Yee, Phys. Rev. Lett. **78**, 1524 (1997).

[30] N. Satomi, A. Takahara, and T. Kajiyama, Macromolecules **32**, 4474 (1999).

[31] B. Jerome and J. Commandeur, Nature (London) **386**, 589 (1997).

[32] F.D. Blum, G. Xu, M. Liang, and C.G. Wade, Macromolecules **29**, 8740 (1996).

[33] W-Y. Lin and F.D. Blum, Macromolecules **30**, 5331 (1997).

[34] D.S. Fryer, P.F. Nealey, and J.J. de Pablo, Macromolecules **33**, 6439 (2000).

[35] Y. Grohens, M. Brogly, C. Lable, M-O. David, and J. Schultz, Langmuir **14**, 2929 (1998).

[36] S.C. Kuebler, D.J. Schaefer, C. Boeffel, U. Pawelzik, and H.W. Spiess, Macromolecules **30**, 6597 (1997).

[37] J. Menegotto, Ph. Demont, and C. Lacabanne, Polymer **42**, 4375 (2001).

[38] S. Doulut, C. Bacharan, P. Demont, A. Bernes, and C. Lacabanne, J. Non-Cryst. Solids **235-237**, 645 (1998).

[39] P.G. de Gennes, Euro. Phys. J. E **2**, 201 (2000).

[40] P.G. de Gennes, C. R. Acad. Sci. IV-Phys. **1**, 1179 (2000).